remote sensing

MDPI

Article

Analysis of Space-Borne GPS Data Quality and Evaluation of Precise Orbit Determination for COSMIC-2 Mission Based on Reduced Dynamic Method

Qiaoli Kong *, Yanfei Chen, Wenhao Fang, Guangzhe Wang, Changsong Li, Tianfa Wang, Qi Bai and Jingwei Han

College of Geodesy and Geomatics, Shandong University of Science and Technology, Qingdao 266590, China; chenyanfei@sdust.edu.cn (Y.C.); sdk993850@sdust.edu.cn (W.F.); wangguangzhe@sdust.edu.cn (G.W.); lcs202083020037@sdust.edu.cn (C.L.); 202083020077@sdust.edu.cn (T.W.); baiqi@sdust.edu.cn (Q.B.); 202183020122@sdust.edu.cn (J.H.)

* Correspondence: qiaolikong@sdust.edu.cn

Abstract: COSMIC-2 is a remote sensing satellite mission that mainly provides scientific data for weather forecasting, ionosphere, and climate research. High precise orbit is the basis for the application of remote sensing satellite data. In order to realize the precise orbit determination (POD) of COSMIC-2, we have assessed the quality of space-borne GPS observation in detail, including the utilization of GPS observations, cycle slip ratio (o/slps), multipath error, single-noise ratio (SNR) and ionospheric delay rate (*IOD*) of the data, realized the POD of COSMIC-2 with the reduced dynamic (RD) method, and evaluated the accuracy of the solved orbit by means of the carrier-phase residual, overlapping orbit comparison and the reference orbit comparison. The data quality assessments show that the data is less affected by the multipath effect, the utilization of the data is low, cycle slips occur frequently, and the carrier-phase data is often interrupted. The POD results indicate that the root mean square (RMS) values of the carrier-phase residuals of six COSMIC-2 satellites are between 6.0 mm and 7.5 mm, The mean RMS values of the overlapping orbit are better than 0.92 cm, 1.33 cm and 1.03 cm in the radial (R), tangential (T) and normal (N) directions respectively, and the mean RMS values of the six satellites in the 3D direction are between 1.38 cm and 1.75 cm. The mean RMS values in R, T and N directions orbit determination accuracy of the reference orbit comparison are better than 5.61 cm, 6.59 cm and 2.29 cm respectively, and the mean RMS values of the six satellites in the 3D direction are between 7.35 cm and 8.79 cm.

Keywords: COSMIC-2; space-borne GPS; quality assessment; reduced dynamic method; precise orbit determination

Citation: Kong, Q.; Chen, Y.; Fang, W.; Wang, G.; Li, C.; Wang, T.; Bai, Q.; Han, J. Analysis of Space-Borne GPS Data Quality and Evaluation of Precise Orbit Determination for COSMIC-2 Mission Based on Reduced Dynamic Method. *Remote Sens.* **2022**, *14*, 3544. https://doi.org/10.3390/rs14153544

Academic Editors: Baocheng Zhang and Teng Liu

Received: 23 June 2022
Accepted: 21 July 2022
Published: 24 July 2022

1. Introduction

FORMAT-7/COSMIC-2 (Constellation Observing System for Meteorology, Ionosphere, and Climate-2 and Formosa Satellite Mission 7) (COSMIC-2) satellite mission was launched on 25 June 2019, started weather forecasting, monitoring and other tasks in February 2020, and completed all orbit adjustment work in May 2021 [1,2]. This is a remote sensing satellite mission jointly developed by the National Space Organization (NSPO), Taiwan and the National Oceanic and Atmospheric Administration (NOAA), USA. It is a continuation of COSMIC-1 mainly used to collect atmospheric data for weather prediction, ionosphere and gravity research [3,4]. COSMIC-2 constellation contains six satellites, the designed orbit inclination is 24 degrees with occultations primarily distributed from 45°N and 45°S, the designed life is 5 years, the initial orbit altitude is 750 km, and the final orbit is 525 km, and it takes about 100 min to fly around the earth per circle [1,5]. In order to realize the scientific function of the constellation and provide the basis for scientific data, each satellite is equipped with the advanced Tri-GNSS radio occultation (RO) system (TGRS) receiver, and its two orbit determination antennas are POD + X and POD − X respectively.

POD + X is located in the satellite flight direction, and POD − X is back in the satellite flight direction [6]. TGRS receiver can track the GPS signal and navigation signal of the GLONASS system, to provide data for the POD of COSMIC-2 [6–8].

At present, there are few studies on the POD of COSMIC-2. Ho et al. (2020) evaluated the neutral atmosphere data quality of COSMIC-2 using the GPS occultation data [9]. Weiss (2021) realized the orbit determination of COSMIC-2 with the RD method, and its 3D orbit determination accuracy was within 10 cm [10]. Jaeggi et al. (2021) solved the orbit of COSMIC-2 with the RD method and found that the accuracy of the overlapping orbits is about 10 cm [11]. Li et al. (2014) carried out orbit determination for COSMIC-1, analyzed the satellite orbit and satellite clock offset, and the 3D orbit determination accuracy was about 10 cm [12]. Hwang et al. (2009) used RD and kinematics to solve the orbit and analyzed the overlapping orbit, the accuracy of the overlapping orbits of the two methods was almost at the same level, both of which were 2–3 cm [13]. Hwang et al. (2006) used the space-borne GPS data of a single antenna to realize the POD of COSMIC-1 by RD and kinematic methods, and the RMS of the average orbit difference between the two methods of satellite FM1-FM6 is 6 cm, and the RMS values of the overlap orbit difference and the orbit difference between the resolved and the reference are about 5 cm and 10 cm, respectively [14]. Kuang et al. (2008) applied GPS data of two antennas to determine the orbit of COSMIC-1, and the three-dimensional accuracy of the orbit was about 6 cm [15]. For the LEO satellite, the required orbit accuracy for COSMIC-2 occultations is about 30 cm [16]. TACC (Taiwan Analysis Center) determined the orbit of COSMIC-2 and used the overlapping orbit comparison method for orbit verification, and the satellite orbit position accuracy was below 15 cm, and the velocity accuracy of the satellite was below 0.15 mm/s (https://tacc.cwb.gov.tw/v2/trops_download.html) (accessed on 12 March 2021). It can be seen that the RD method is mostly used for orbit determination of COSMIC satellite missions, and the 3D orbit accuracy is about 10 cm. There are mainly three POD methods such as kinematic, dynamic and RD methods. The kinematic method is based on PPP (precise point positioning) using GNSS data [17–19] and the dynamic one is mainly based on the dynamic models, while the RD method has combined the advantages of the first two methods. Therefore, we also apply the RD method to carry out POD for COSMIC-2.

Due to the small amount of GLONASS data received by POD − X [1], all tests in this study are based on GPS data of the rear POD (POD − X) antenna, and the main purpose of this paper is to carry out a detailed quality assessment of the space-borne GPS data for six COSMIC-2 satellites, and realize the POD with the RD method, and evaluate the orbit accuracy by carrier-phase observation residual, overlapping orbits comparison and reference orbit comparison. Section 2 introduces the content of data quality analysis in detail, including the utilization of GPS observations, cycle slip ratio (o/slps), multipath error, SNR and *IOD*. Section 3 shows the relevant theories of the reduced dynamic method and the orbit determination strategy of six COSMIC-2 satellites, determines the orbit of COSMIC-2 with the reduced dynamic and evaluates the orbit accuracy using the carrier-phase residual, overlapping arcs comparison and the reference orbit comparison. Section 4 gives the relevant conclusions.

2. Quality Assessment of COSMIC-2 GPS Observations

In this study, the GPS observation data of the COSMIC-2 satellite rear antenna (−X (rear) POD antenna) provided by the Central Weather Bureau, Taiwan (https://tacc.cwb.gov.tw/) (accessed on 12 March 2021) are used. The time length of observation data is five days from 18 to 22 May 2021 (day of the year (DOY) 138–142), and the GPS precise ephemeris and GPS satellite clock error files applied are downloaded from CODE (http://ftp.aiub.unibe.ch/CODE/) (accessed on 12 March 2021) with 15 min and 30 s sampling interval, respectively. The structure of COSMIC-2 is shown in Figure 1 [1].

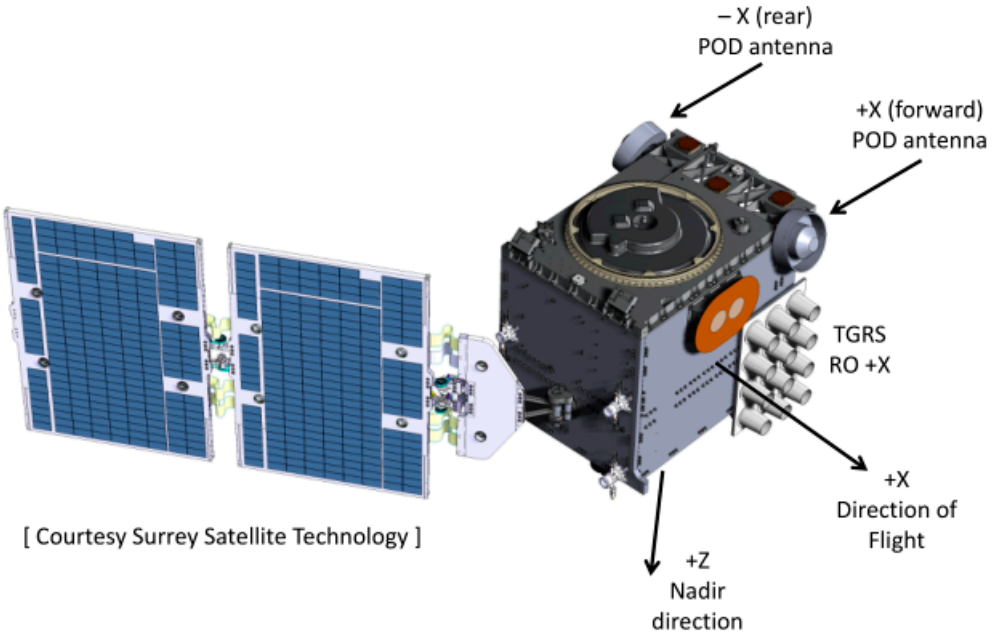

Figure 1. Satellite Structure of COSMIC-2.

LEO satellites move at high speed in space and are susceptible to the influence of the complex surrounding environment, and the quality of observation data is the key to the accuracy of satellite orbit determination. Therefore, it is essential to analyze the quality of observation data. The main factors affecting the quality of observation data include the visibility of GNSS satellites, the utilization of GPS observations, cycle slip ratio, SNR (SNR1, SNR2), multipath effect error (*MP*1, *MP*2) and *IOD* [20–22]. SNR1 and SNR2, and *MP*1 and *MP*2 are SNR and multipath errors on L1 and L2 frequencies respectively. The ratio of the total number of observations to the number of observations with cycle slip is called the cycle slip ratio, which reflects the situation of data cycle slips. The larger the ratio is, the fewer slips occur, and vice versa. The integrity of data reflects the performance of the space-borne GPS receiver and the observation environment [23]. In order to assess the quality of COSMIC-2 space-borne GPS data, the above indexes are studied in detail by the public software TEQC [24]. There are a large number of missing data for the two days of DOY140 and DOY141 for Sat–1, so the quality assessment of the data of Sat–1 on these two days will not be carried out.

2.1. GPS Satellite Visibility

The visibility of the GPS satellites of six COSMIC-2 satellites on DOY 138 is shown in Figure 2. The statistical information on the percentage of visible satellites of DOY 138–142 is listed in Table 1.

Table 1. Percentage statistics of the visible number of GPS satellites for the six COSMIC-2 satellites, DOY 138–142, 2021.

	≤3 (%)	4~6 (%)	7~10 (%)	≥11 (%)	Mean (Number)
Sat–1	0.10	18.50	81.17	0.23	7.56
Sat–2	0.10	20.44	79.24	0.22	7.54
Sat–3	0.20	15.57	83.80	0.42	7.67
Sat–4	0.36	18.56	81.04	0.03	7.55
Sat–5	0.30	12.90	86.12	0.68	7.71
Sat–6	0.05	16.42	83.16	0.38	7.60

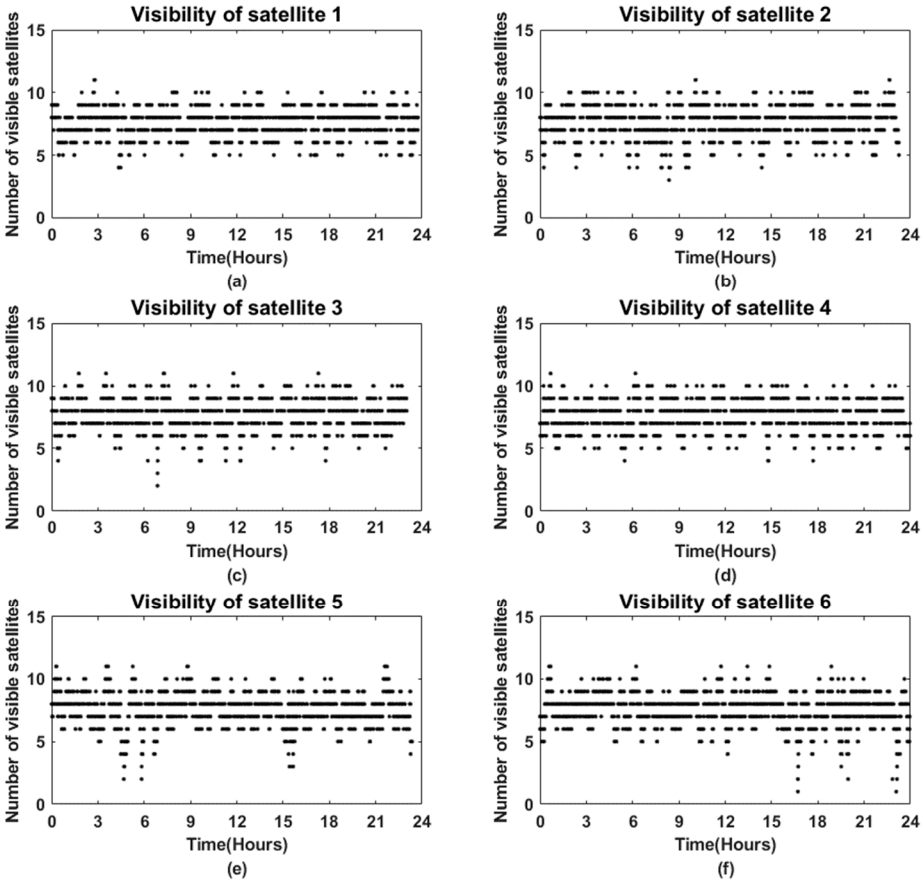

Figure 2. Numbers of visible GPS satellites of six COSMIC-2 satellites, DOY 138, 2021 ((**a**–**f**) are visibility of satellite 1~6 respectively).

As seen in Figure 2 and Table 1, the number of GPS satellites tracked by the space-borne GPS receiver is mostly in the range of 7–10, and there are few epochs with the number of the tacked GPS satellite below 3. The average number of visible satellites for all six COSMIC-2 satellites is larger than 7, which indicates that the space-borne GPS receiver has a good observation performance.

2.2. Utilization of GPS Observations

Data utilization refers to the ratio of the actual epochs of data to the theoretical epochs, which is defined as follows:

$$\eta = \frac{n_h}{n_e} \tag{1}$$

where n_h is the actual number of epochs, n_e is the number of theoretical epochs. This indicator can reflect the utilization of observation data and the observation environment around the receiver [25]. Table 2 shows the utilization of the observed data of six COSMIC-2 satellites of DOY 138–142.

Table 2. Utilization of GPS observations of COSMIC-2, DOY 138–142, 2021 (%).

DOY	Sat–1	Sat–2	Sat–3	Sat–4	Sat–5	Sat–6	Mean
138	27	33	28	28	27	28	29
139	26	35	30	27	30	28	29
140	31	32	30	37	27	27	31
141	43	30	34	38	33	28	34
142	28	31	29	34	30	27	30
Mean	31	32	30	33	29	28	—

From Table 2, it can be seen that the highest average observation efficiency is in DOY 141, and the observation efficiency of Sat–4 is relatively higher than that of other COSMIC-2 satellites in DOY 138–142. It can be seen that the effectiveness rate of COSMIC-2 space-borne observation data is lower than 40%, which indicates that the quality of the observation environment around the receiver is not well.

2.3. Cycle Slip Ratio

The cycle slip ratio is the ratio of the total number of actual observations to the number of cycle slips, which is used to explain the cycle slip of observation data. The satellite receiver is moving at high-speed. Due to the fast speed of satellite movement, the poor space environment of the satellite receiver, the influence of the multipath effect and other reasons, it will cause the discontinuity of observation data or the loss of lock of GPS signal, resulting in a cycle slip of observation data [26]. The larger the cycle slip ratio is, the less the cycle slip occurs in the data, and vice versa. The statistical information of the cycle slip ratio of the observation of six COSMIC-2 satellites is listed in Table 3.

Table 3. Cycle slip ratio of observation of COSMIC-2, DOY 138–142, 2021.

DOY	Sat–1	Sat–2	Sat–3	Sat–4	Sat–5	Sat–6	Mean
138	7	9	8	8	7	7	8
139	8	10	9	9	8	8	9
140	7	10	9	9	6	7	8
141	10	10	11	9	8	7	9
142	8	11	11	10	9	7	9
Mean	8	10	10	9	8	7	—

Table 3 indicates that the average cycle slip ratio of DOY 138–142 is 8 or 9, and the cycle slip ratio of six COSMIC-2 satellites is generally lower than that of the receiver on the surface of the Earth. Sat–2 and Sat–3 own the highest cycle slip ratio among the six COSMIC-2 satellites, with a ratio of 10, and Sat–6 owns the lowest one, with a ratio of 7. The above analysis shows that the frequency of cycle slips of COSMIC-2 during the observation period is large, and the number of cycle slips is large.

2.4. Single Noise Ratio

The signal-noise ratio (SNR) is the ratio of the carrier signal intensity received in the receiver to the noise intensity. That can reflect the signal quality of the carrier. The higher the SNR is, the smaller the error is [27]. In the process of TEQC detection, SNR1 and SNR2 are the average signal-noise ratios on L1 and L2 carriers respectively, and the thresholds are set to 6 and 4 respectively [28,29]. The mean SNR of every COSMIC-2 satellite every day and the mean SNR of six COSMIC-2 satellites every day in 5 days is plotted in Figures 3 and 4 respectively.

As can be seen from Figures 3 and 4, both SNR1 and SNR2 of the six COSMIC-2 satellites for 5 days are much larger than the threshold value, the SNR is relatively smooth, and there is no significant fluctuation, besides, SNR1 is somewhat larger than SNR2, which indicates that the signal quality of L1 is better than that of L2.

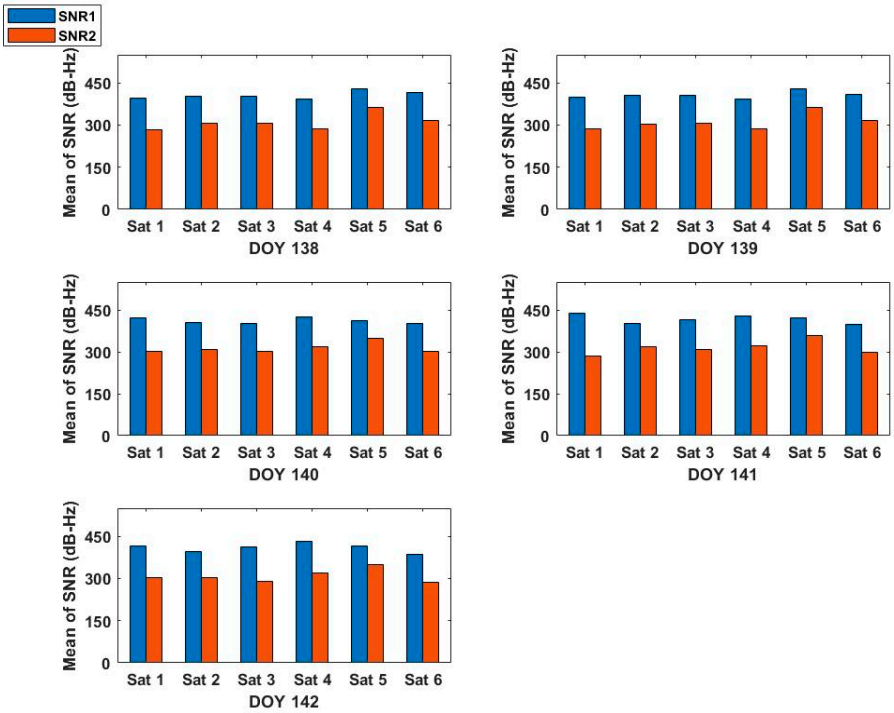

Figure 3. Mean SNR of each COSMIC-2 satellite during DOY 138–142, 2021.

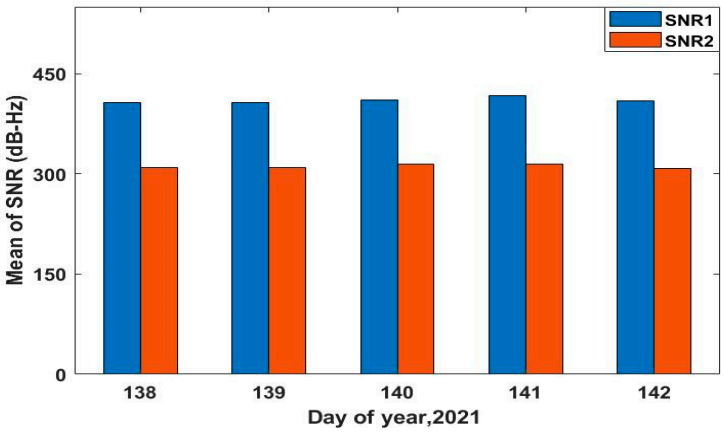

Figure 4. Mean SNR of six COSMIC-2 satellites during DOY 138–142, 2021.

2.5. Multipath Effect

In the process of satellite signal propagation, due to the influence of the surrounding environment, the signal of the surrounding reflectors will enter the receiver with the satellite signal, resulting in a deviation between the observed value and the true value, this phenomenon is called multipath effect [30–32]. The multipath error is mainly due to pseudo-ranges and can be determined by the linear combination of pseudo-range and phase observations, and its calculation formula is:

$$MP1 = P_1 - (1 + \frac{2}{\alpha - 1})\varphi_1 + (\frac{2}{\alpha - 1})\varphi_2 \quad (2)$$

$$MP2 = P_2 - (\frac{2\alpha}{\alpha - 1})\varphi_1 + (\frac{2}{\alpha - 1} - 1)\varphi_2 \quad (3)$$

where $MP1$ and $MP2$ are multipath errors on L1 and L2 bands respectively, $\alpha = \frac{{f_1}^2}{{f_2}^2}$ (f_1 and f_2 are the frequency values of L1 and L2 bands respectively), P_1, P_2 are pseudo-range observations and φ_1, φ_2 are the phase observations on both frequencies, respectively.

The thresholds of RMS for *MP*1 and *MP*2 in TEQC are set as 0.5 m and 0.75 m respectively, and the smaller RMS indicates that the observed data are less affected by multipath effects [28,33]. The mean multipath errors of every COSMIC-2 satellite are plotted every day in Figure 5, and the mean multipath error of six COSMIC-2 satellites every day over 5 days is shown in Figure 6.

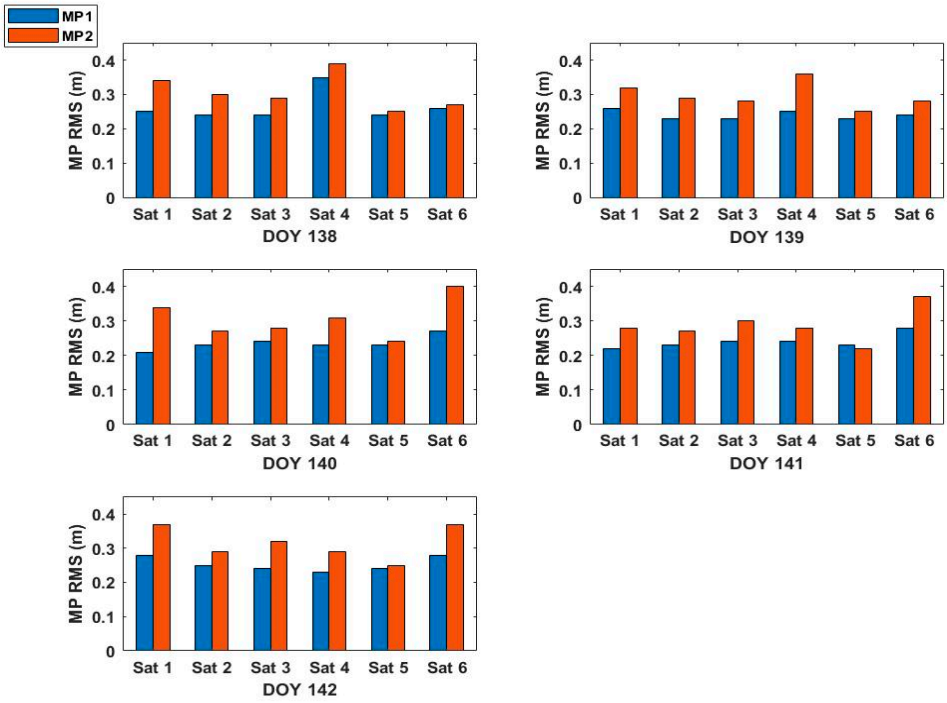

Figure 5. Multipath errors of each COSMIC-2 satellite during DOY 138–142, 2021.

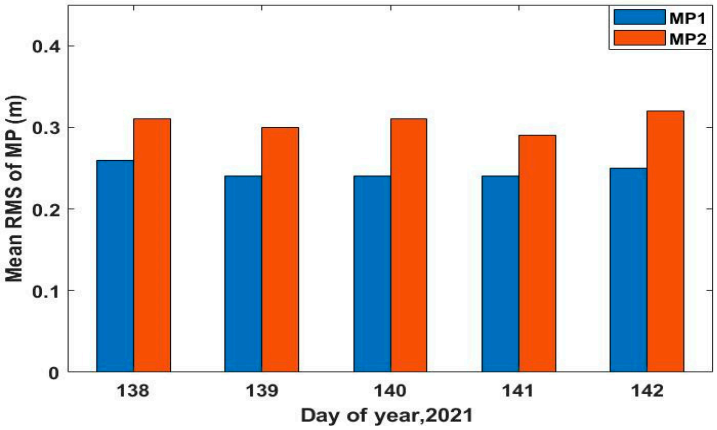

Figure 6. Mean multipath errors of six COSMIC-2 satellites during DOY 138–142, 2021.

As can be seen from Figures 5 and 6, the RMS of *MP*1 and *MP*2 of these satellites are within the index value range. Among them, the RMS of *MP*1 is generally less than *MP*2, except for Sat–5 in DOY 141, but it is still within the limit, so it has little impact on data quality.

2.6. Ionospheric Delay Rate

The change rate of ionospheric delay refers to the change of ionospheric delay in unit time [34]. Influenced by the ions in the ionosphere, the propagation speed and propagation path of the signals emitted by GPS satellites change as they pass through the ionosphere, which has an effect on the time of signal propagation, thus changing the geometric distance

between the source and the receiver [30]. The ionospheric delays on the L1 and L2 carriers are obtained by making a difference between the dual-frequency carrier-phase observations, assuming that the carrier waves of both frequencies have the same propagation path in the atmosphere [26]:

$$I_1 = \frac{1}{\alpha - 1}(\lambda_1\varphi_1 - \lambda_2\varphi_2 - n_1\lambda_1 + n_2\lambda_2) \quad (4)$$

$$I_2 = \frac{\alpha}{\alpha - 1}(\lambda_1\varphi_1 - \lambda_2\varphi_2 - n_1\lambda_1 + n_2\lambda_2) \quad (5)$$

where, φ_1, φ_2 are the phase observations. IOD is computed in TEQC as follows [30]:

$$IOD = \frac{\alpha}{\alpha - 1}[(L_1 - L_2)_i - (L_1 - L_2)_{j-1}]/(t_j - t_{j-1}) \quad (6)$$

when $IOD \geq 400$ cm/min, it is considered that the ionosphere jumps [25,35,36]. If the data of a whole day is selected, the 24-h window will make the image too dense to clearly display the changes. Therefore, the time period of 21:00:00–21:59:59 of Sat–2 is selected to analyze the ionospheric delay change rate, as shown in Figure 7.

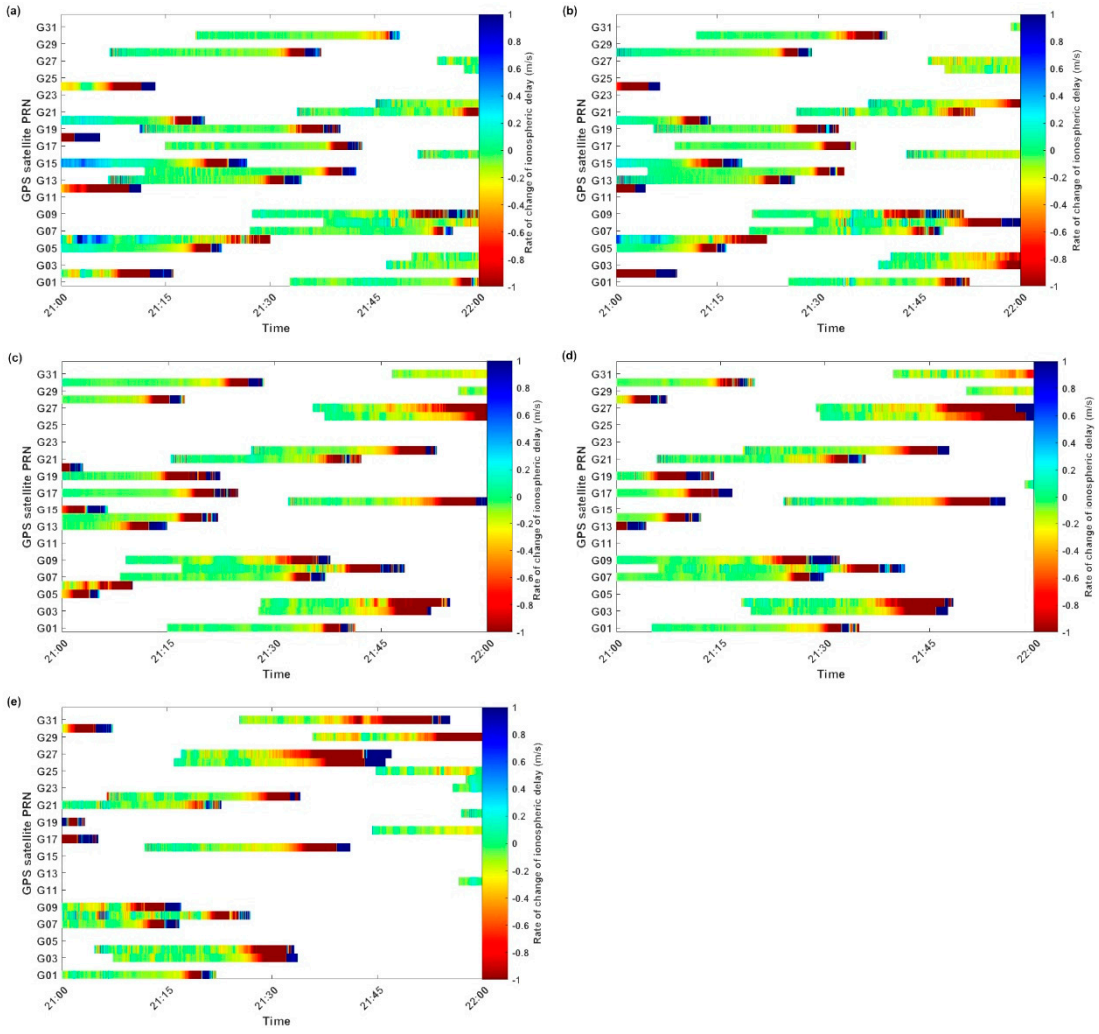

Figure 7. Ionospheric delay rate of Sat–2 ((**a**–**e**) are DOY 138–142 respectively).

It can be seen from Figure 7, where when no cycle slips are present, the IOD is quite smaller than 400 cm/min [36], that since at the 500 km~525 km (height of the COSMIC-2), the observed ionosphere effect is only a small fraction of the total effect. It is also apparent from Figure 7, the IOD increases significantly at the end of the data acquisition cycle. And

that the main reason for this phenomenon is the discontinuity of carrier phase data and the emergence of abnormal values [37].

From the above GPS data quality analysis, it can be seen that the number of the visible GPS satellites of six COSMIC-2 satellites in the five days is mostly 7–10, and there are few epochs with the number of the tacked GPS satellite below 3; The low utilization of observations indicates that the quality of the surrounding observation environment is not high; The average cycle slip ratios of five days is relatively low, which indicates that the frequency of cycle slip of COSMIC-2 is high and the number of cycle slips is large during the observation period; In terms of SNR, the average value of six COSMIC-2 satellites is more than 300, and SNR1 and SNR2 are far greater than the threshold. In terms of multipath error, the RMS of $MP1$ and $MP2$ of COSMIC-2 are within the index value range, indicating that the satellite signal is less subject to multipath interference. In terms of IOD, it is obviously found that the IOD changes greatly at the end of the data acquisition cycle, mainly due to the discontinuity of carrier-phase data and the emergence of outliers. Generally speaking, the GPS observation data quality of DOY 138–142, for five days, is general, the data loss is serious, and the cycle slip occurs frequently, but its signal-noise ratio is high, and the error caused by the multipath effect is small.

3. Reduced Dynamic Orbit Determination of COSMIC-2

3.1. Reduced Dynamic Method

LEO satellites are affected by various perturbations when they move around the earth, including conservative forces and non-conservative forces. The conservative forces mainly include non-spherical gravitation perturbations, multi-body perturbation, earth tide perturbation, relativistic effects, and non-conservative forces include solar radiation pressure, earth's albedo, and atmospheric drag force. The motion equation of an LEO satellite considering these perturbations in the geocentric inertial system is [30,38]:

$$\ddot{r} = -GM\frac{r}{r^3} + f_1(t, \dot{r}, \ddot{r}, q_1 \ldots, q_d) \tag{7}$$

where: $r, \dot{r}, \ddot{r}$ are the position, velocity and acceleration of the satellite, respectively; The initial condition is $r_0(t) = r(a, e, i, \Omega, \omega, T_0; t_0)$, $\dot{r}(t_0) = \dot{r}(a, e, i, \Omega, \omega, T_0; t_0)$, Where, $(a, e, i, \Omega, \omega, T_0; t_0)$ are Kepler six elements at the reference epoch t_0; f_1 is disturbance acceleration; $q_1 \ldots, q_d$ are the unknown dynamic orbit parameters; GM is the gravitational constant of the earth.

Assuming that the prior orbit $r_0(t)$ of the satellite is known, the Taylor series expansion of $r(t)$ is carried out at the reference epoch t_0 to eliminate the unknown disturbing force parameters. The corrected value of the prior orbit parameter p_{i0} is obtained in the least square processing of GPS carrier-phase observation data of the LEO satellite. The expression of the final orbit $r(t)$ is [38]:

$$r(t) = r_0(t) + \sum_{i=1}^{n} \frac{\partial r_0(t)}{\partial p_i}(p_i - p_{i0}) \tag{8}$$

where: p_i is the track parameter; p_{i0} is a priori orbit parameter.

LEO satellites will be affected by atmospheric drag force when they move around the earth. Due to the complex space environment, it is difficult to model the atmospheric drag force. Therefore, the un-modelled atmospheric drag force will degrade the orbit determination accuracy with the dynamic method [39]. The RD orbit determination method is to introduce pseudo-random pulse parameters into the satellite motion equations, adopts the geometric information of the GPS observations and the dynamic information of the satellite, and balances the geometric and kinematic information by a priori weights [39,40]. A priori weight can keep the pseudo-random pulse parameters from deviating from the expected value, and it can effectively absorb the dynamic model errors and the un-modelled perturbation errors, so as to improve the RD orbit determination accuracy for LEO satellites [4,39].

3.2. Orbit Determination Strategy for COSMIC-2

In this study, the RD method POD for six COSMIC-2 satellites with five-day spaceborne GPS observation is carried out with Bernese 5.2 software [41]. The orbit determination arc section is 24 h. Due to the serious lack of observation data on DOY 140 and DOY 141 of Sat–1, the orbits of this satellite in these two days are not solved. In order to evaluate the accuracy of the solved orbits of COSMIC-2 using the RD method, three orbit accuracy analysis methods are applied, these three methods include the analysis of carrier-phase observation residuals, and the comparison of overlapping orbits and the comparison with reference orbits. The orbit determination strategy is shown in Table 4.

Table 4. RD orbit determination strategies of COSMIC-2.

Models/Parameters	Description
Mean earth gravity	EGM2008_SMALL
N-body	JPL DE405
Relativity	IERS2010XY
Ocean Tides	FES2004
Solid-earth tides	TIDE2000
GPS precise ephemeris	ftp://ftp.aiub.unibe.ch/CODE (accessed on 12 March 2021)
GPS precise clock offset	ftp://ftp.aiub.unibe.ch/CODE (accessed on 12 March 2021)
Antenna PCO and PCV	Igs14.atx
Elevation cutoff	5°
Sampling interval	10 s
Pseudostochastic pulses	6 min
Arc length of orbit determination	24 h

3.3. Assessment of Orbit Accuracy

In this study, the accuracy validation methods of the RD orbit of COSMIC-2 include internal validation and external validation. The former is carried out by carrier-phase residuals and overlapping orbit comparison, and the latter is performed by comparison with the reference orbit.

3.3.1. Analysis of Carrier-Phase Residuals

The carrier-phase residuals mainly contain the modelled and un-modelled errors, and the RMS of the residuals can, to a certain extent, reflect the set strategies and whether selected mechanics models are suitable or not, so the RMS of the residuals can be used as one of the indicators for the evaluation of the internal conformity accuracy of POD [42]. The smaller the RMS of the residual is, the higher the accuracy of the internal conformity is. Table 5 shows the statistical results of the RMS of the carrier-phase residuals for the six COSMIC-2 satellites with the RD orbit determination method for each day from 18–22 May 2021 (DOY 138–142).

Table 5. Statistical results of RMS of carrier-phase residuals (mm).

DOY	Sat–1	Sat–2	Sat–3	Sat–4	Sat–5	Sat–6
138	6.4	6.0	6.4	7.0	6.6	6.6
139	6.7	6.2	6.3	6.0	6.7	7.0
140	—	6.5	6.6	6.3	6.8	6.8
141	—	6.4	6.9	6.2	6.7	7.2
142	6.1	6.6	6.0	6.2	6.5	7.5
Mean	6.4	6.0	6.4	7.0	6.6	6.6

It can be seen from Table 5 that the RMS values of the carrier-phase residuals of the six COSMIC-2 satellites vary between 6.0 mm and 7.5 mm, and the mean RMS values of the residual for Sat–2 in the five days is the smallest and that of Sat–4 is the largest. The

mean residual RMS values of the six COSMIC-2 satellites in DOY 138–142 vary between 6.0 mm and 7.0 mm, which indicates that the observations measured by the space-borne GPS receiver are relatively stable.

3.3.2. Overlap Orbit Validation

In order to evaluate the orbit determination accuracy for the six satellites using the overlap validation method, two-orbit determination arc sections are set every day, and the time spans are 00:00:00–17:59:59 and 12:00:00–23:59:59 respectively. The overlap time is 6 h. Although the observations of the two overlapping orbits are the same, the two orbits are solved by two independent orbit determination processes [43]. Therefore, the overlapping orbits of the two orbit determination arcs for 6h are not related to each other. In order to avoid the boundary effect, the overlapping arc of 4h from 13:00:00 to 16:59:59 are selected for comparison [39,44]. The overlapping orbit difference of six COSMIC-2 satellites in R, T and N directions is shown in Figure 8, and the mean RMS values of orbit difference between overlapping orbits during DOY 138–142 are given in Table 6.

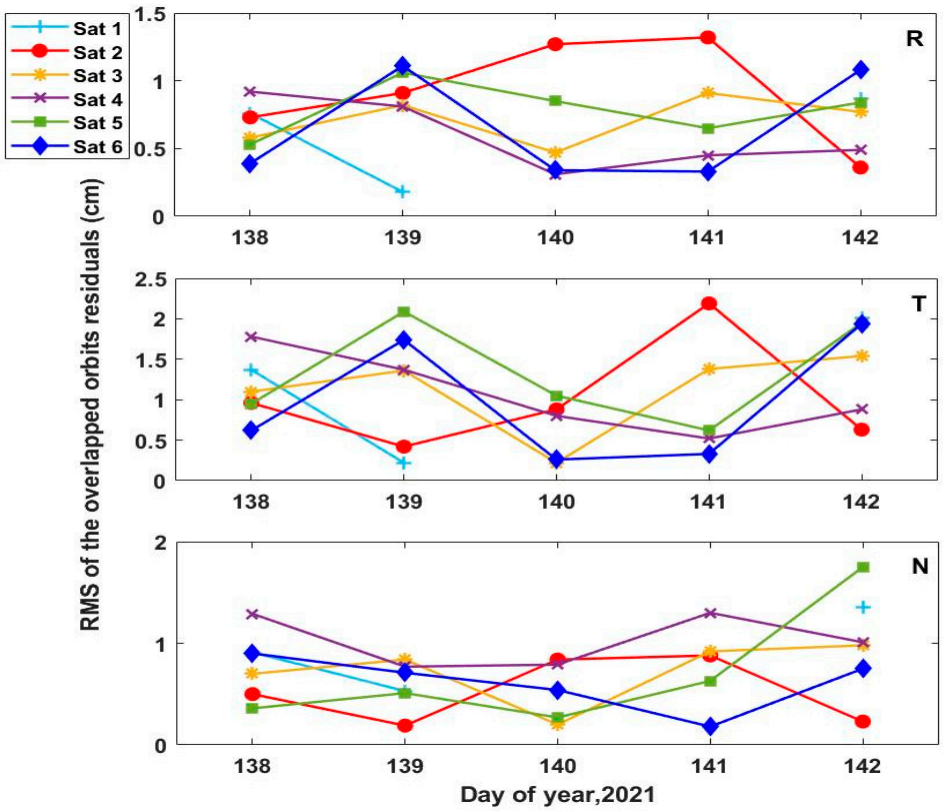

Figure 8. RMS of differences between overlapping orbits for COSMIC-2.

Table 6. Mean RMS of differences between overlapping orbits for COSMIC-2 (cm).

	R	T	N	3D
Sat–1	0.60	1.20	0.93	1.66
Sat–2	0.92	1.02	0.53	1.51
Sat–3	0.71	1.12	0.73	1.53
Sat–4	0.60	1.07	1.03	1.64
Sat–5	0.79	1.33	0.70	1.75
Sat–6	0.65	0.98	0.62	1.38

It can be seen from Figure 8 that the RMS values in the R, T and N directions of the 4 h overlapping orbit difference in the five days are smaller than 3 cm, and the RMS in the T direction is significantly larger than that in R and N directions. Table 6 and Figure 8

show that the mean RMS values of the overlapping orbit differences of the six COSMIC-2 satellites during DOY 138–142 fluctuate between 1.38 cm and 1.75 cm in the 3D direction, and the mean RMS of Sat–6 in the 3D direction is the smallest and that of Sat–5 in the 3D direction is the largest. The overlapping orbit validation indicates that mean the RMS values in 3D of the six COSMIC-2 satellites are all better than 2 cm. Obviously, our orbit determination accuracy is higher than that of TACC of 15 cm, and the result meets the orbit determination accuracy requirements of COSMIC-2.

3.3.3. Validation with Reference Orbits

In this study, we carried out an orbit comparison between the resolved orbits with the RD method and the reference orbit released by Central Weather Bureau and evaluated the external coincidence accuracy of the RD orbit according to the RMS values of the differences between them. The RMS values of differences between the RD orbits and external reference orbits during DOY 138–142 are shown in Figure 9, and the corresponding mean RMS values for each day are shown in Table 7.

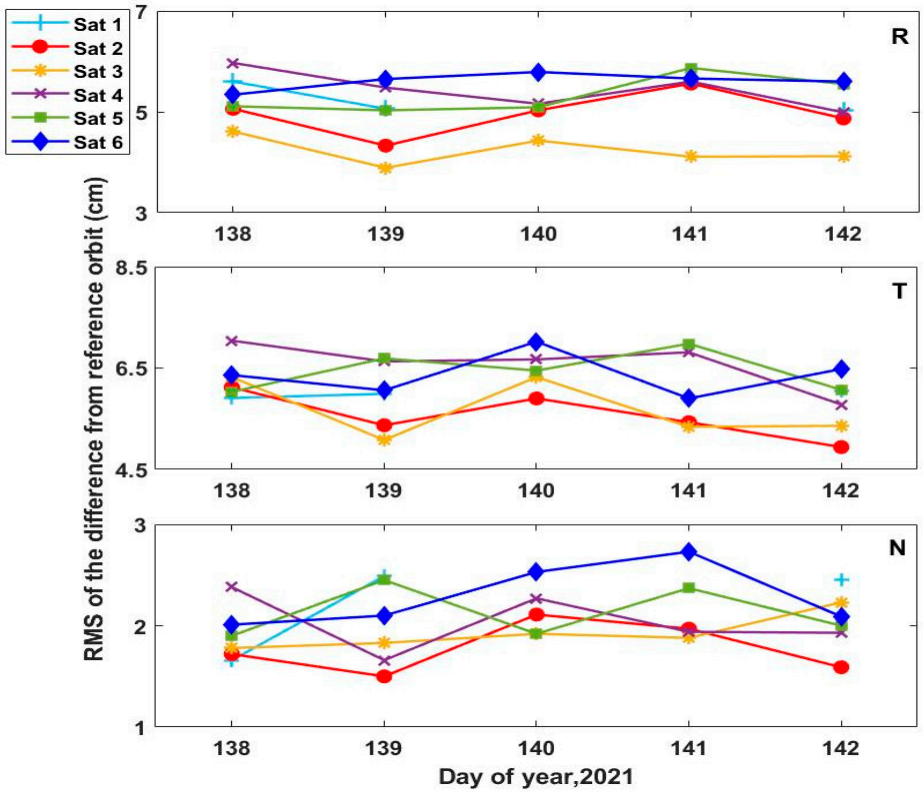

Figure 9. RMS of difference between the solved orbits and the reference ones.

Table 7. Mean RMS of difference between the solved orbits and the reference ones (cm).

	R	T	N	3D
Sat–1	5.23	5.98	2.20	8.26
Sat–2	4.97	5.55	1.78	7.67
Sat–3	4.23	5.68	1.93	7.35
Sat–4	5.44	6.59	2.04	8.79
Sat–5	5.33	6.44	2.13	8.64
Sat–6	5.61	6.36	2.29	8.79

It can be seen from Table 7 and Figure 9 that the mean RMS values of the orbit differences of the six COSMIC-2 satellites fluctuate between 7.35 cm and 8.79 cm during DOY 138–142 in the 3D direction, and the mean RMS value of Sat–3 in the 3D direction

is the smallest and the ones of Sat–4 and Sat–6 are 8.79 cm, which is the largest among the six satellites. The orbit difference of the six COSMIC-2 satellites in the N direction in these five days is smaller than that in the T and R directions. The mean RMS of difference between the RD orbit and the reference orbit of DOY 138–142 for five days are below 5.61 cm, 6.59 cm and 2.29 cm in R, T and N directions, respectively. The mean RMS of 3D of the six COSMIC-2 satellites is better than 9 cm, which meets the orbit determination accuracy requirements of COSMIC-2.

4. Conclusions

This paper focuses on evaluating the space-borne GPS data and achieving POD for COSMIC-2. Based on TEQC, the observation data quality evaluation for COSMIC-2 was carried out from aspects of satellite visibility, utilization of GPS observations, SNR, cycle slip ratio, multipath error and IOD. The results show that the proportion of 7–10 GPS satellites tracked by the six space-borne GPS receivers in each epoch is more than 79%, the average value of SNR is greater than 300, the data is less affected by the multipath effect, and SNR1 is better than SNR2 in signal-noise ratio. However, it is found that the utilization of the observation data is low and cycle slips occur frequently. The analysis of the change rate of ionospheric delay proves that the carrier-phase data is often interrupted.

The POD was carried out based on the RD method using the five-day space-borne GPS observation of COSMIC-2, and the accuracy of the solved orbit is evaluated by three methods: carrier-phase residual analysis, overlapping orbit comparison and reference orbit comparison. (1) According to the residual analysis of carrier-phase observations, it is found that the residual RMS of carrier-phase observations for the RD orbit determination of six COSMIC-2 satellites is between 6.0 mm and 7.5 mm. (2) 4 h overlapping orbits are compared, and the test results show that the RMS values of the differences between the 4 h overlapping orbits in the three directions of R, T and N in five days are below 3 cm, and the mean RMS of six COSMIC-2 satellites in 3D are better than 2 cm, which indicates that this result is better than the overlapping orbit verification accuracy released by TACC. (3) According to the comparison between the solved orbit and the reference orbit, the results show that the RMS values of the orbit differences between the above two orbits of the six COSMIC-2 satellites in the R, T and N directions are all within 8 cm, and the mean RMS values of the 3D of the six COSMIC-2 satellites are smaller than 9 cm, which meets the orbit determination accuracy requirements of COSMIC-2. It can be seen that we have achieved the POD for COSMIC-2, and the orbit determination results can meet the requirements of the application of its science data.

Author Contributions: Conceptualization, writing—original draft preparation, writing—review and editing and methodology, Q.K., Y.C. and W.F.; software, Y.C.; validation, Y.C. and W.F.; data curation, G.W., C.L. and T.W.; formal analysis, J.H. and Q.B.; funding acquisition, Q.K. All authors have read and agreed to the published version of the manuscript.

Funding: This work was supported by the National Natural Science Foundation of China (Grant No. 41704015, 41774001), the Shandong Natural Science Foundation of China (Grant No. ZR2017MD032, ZR2021MD030), a Project of Shandong Province Higher Education Science and Technology Program (Grant No. J17KA077), Talent introduction plan for Youth Innovation Team in universities of Shandong Province (innovation team of satellite positioning and navigation).

Data Availability Statement: Our sincere thanks go to the Central Weather Bureau for providing space-borne GPS data for COSMIC-2; CODE Analysis Center at AIUB for providing GPS satellite orbits, clocks and Earth rotation parameters.

Acknowledgments: We thank the Astronomical Institute of the University of Bern (AIUB) for providing Bernese GNSS Software, and the UNAVCO Facility for providing TEQC Software.

Conflicts of Interest: The authors declare no conflict of interest.

References

1. Weiss, J.P.; Hunt, D.; Schreiner, W.; Vanhove, T.; Arnold, D.; Jaeggi, A. COSMIC-2 Precise Orbit Determination Results. In Proceedings of the EGU General Assembly Conference Abstracts, Vienna, Austria, 3–8 May 2020; p. 20170. [CrossRef]
2. Xue, Z.Y. Quality Evaluation of COSMIC-2 Occultation Atmospheric Profile Inversion and Research on Boundary Layer Height Inversion Method. Master's Thesis, Nanjing University of Information Engineering, Nanjing, China, 2021. [CrossRef]
3. Cook, K.; Fong, C.J.; Wenkel, M.J.; Wilczynski, P.; Yen, N.; Chang, G.S. COSMIC-2/FORMOSAT-7: The future of global weather monitoring and prediction. In Proceedings of the 2015 IEEE Aerospace Conference, Pasadena, CA, USA, 7–14 March 2015; pp. 1–11. [CrossRef]
4. Qin, J.; Guo, J.Y.; Kong, Q.L. Precise orbit determination of Jason-2 with the precision of centimeters based on space-borne GPS technique. *Geo. Inform. Sci. Wuhan Univ.* **2014**, *39*, 137–141. [CrossRef]
5. Liu, J.Y.; Lin, C.Y.; Tsai, H.F. Electron density profiles probed by radio occultation of FORMOSAT-7/COSMIC-2 at 520 and 800 km altitude. *Atmos. Meas. Technol.* **2015**, *8*, 3069–3074. [CrossRef]
6. Guo, J.Y.; Huang, J.W.; Zeng, Z.B.; Chang, X.T.; Han, Y.B. Study on geometric orbit determination of COSMIC satellite based on GPS non-difference data. *Prog. Nat. Sci.* **2008**, *1*, 75–80. Available online: https://kns.cnki.net/kcms/detail/detail.aspx?FileName=ZKJZ200801011&DbName=CJFQ2008 (accessed on 10 March 2021).
7. Cherniak, I.; Zakharenkova, I.; Braun, J.; Wu, Q.; Pedatella, N.; Schreiner, W.; Schreiner; Weiss, J.; Hunt, D. Accuracy assessment of the quiet-time ionospheric F2 peak parameters as derived from COSMIC-2 multi-GNSS radio occultation measurements. *J. Space. Weather. Spac.* **2021**, *11*, 18. [CrossRef]
8. Adhikari, L.; Ho, S.P.; Zhou, X. Inverting COSMIC-2 phase data to bending angle and refractivity profiles using the full spectrum inversion method. *Remote Sens.* **2021**, *13*, 1793. [CrossRef]
9. Ho, S.P.; Zhou, X.; Shao, X.; Zhang, B.; Adhikari, L.; Kireev, S.; He, Y.X.; Lynch, E. Initial assessment of the COSMIC-2/FORMOSAT-7 neutral atmosphere data quality in NESDIS/STAR using in situ and satellite data. *Remote Sens.* **2020**, *12*, 4099. [CrossRef]
10. Weiss, J.P. Recent Precise Orbit Determination Results for the COSMIC-2 Mission. In Proceedings of the 43rd COSPAR Scientific Assembly, Online Confernece, Australia, 28 January–4 February 2021; Volume 43, p. 2337. Available online: https://ui.adsabs.harvard.edu/abs/2021cosp...43E2337W/abstract (accessed on 10 March 2021).
11. Jaeggi, A.; Arnold, D.; Weiss, J.; Hunt, D. Assessment of COSMIC-2 reduced-dynamic and kinematic orbit determination. In Proceedings of the EGU General Assembly, Vienna, Austria, 25–30 April 2021. [CrossRef]
12. Li, Y.; Hwang, C.; Tseng, T.; Huang, C.; Bock, H. A Near-Real-Time Automatic Orbit Determination System for COSMIC and Its Follow-On Satellite Mission: Analysis of Orbit and Clock Errors on Radio Occultation. *IEEE T. Geosci. Remote.* **2014**, *52*, 3192–3203. [CrossRef]
13. Hwang, C.; Tseng, T.; Lin, T.; Svehla, D.; Schreiner, B. Precise orbit determination for the FORMOSAT-3/COSMIC satellite mission using GPS. *J. Geod.* **2009**, *83*, 477–489. [CrossRef]
14. Hwang, C.; Tseng, T.; Lin, T.; Fu, C.; Svehla, D. Precise Orbit Determination for FORMOSAT-3/COSMIC and Gravity Application. In Proceedings of the AGU Fall Meeting Abstracts, San Francisco, CA, USA, 11–15 December 2006. Available online: https://ui.adsabs.harvard.edu/abs/2006AGUFM.A14A..04H/abstract (accessed on 10 March 2021).
15. Kuang, D.; Bertiger, W.; Desai, S.; Haines, B.J.; Iijima, B.A.; Meehan, T.K. Precise orbit determination for COSMIC satellites using GPS data from two on-board antennas. In Proceedings of the 2008 IEEE/ION Position, Location and Navigation Symposium, Monterey, CA, USA, 5–8 May 2008; pp. 720–730. [CrossRef]
16. William, M.; Melbourne; Liu, Y.C. *Radio Occultation Using Earth Satellites: A Wave Theory Approach*; Tsinghua University Press: Beijing, China, 2011.
17. Zhang, B.C.; Chen, Y.C.; Yuan, Y.B. PPP-RTK based on undifferenced and uncombined observations: Theoretical and practical aspects. *J. Geo.* **2018**, *93*, 1011–1024. [CrossRef]
18. Zhang, B.C.; Hou, P.; Zha, J.P.; Liu, T. Integer-estimable FDMA model as an enabler of GLONASS PPP-RTK. *J. Geo.* **2021**, *95*, 91. [CrossRef]
19. Zhang, B.C.; Hou, P.; Zha, J.P.; Liu, T. PPP-RTK functional models formulated with undifferenced and uncombined GNSS observations. *Satell. Navig.* **2022**, *3*, 3. [CrossRef]
20. Braasch, M.S. Isolation of GPS Multipath and Receiver Tracking Errors. *Annu. Navig.* **1994**, *41*, 415–434. [CrossRef]
21. Li, Z.H.; Huang, J.S. *GPS Surveying and Data Processing*, 3rd ed.; Wuhan University Press: Wuhan, China, 2005; pp. 99–129.
22. Guo, J.Y.; Zong, G.; Li, W. Classification Solution of Single-Epoch Ambiguity and Ionospheric Delay for Single GPS Satellite. *J. Shandong Univ. Sci. Technol.* **2015**, *34*, 54–60. [CrossRef]
23. Fan, S.J.; Guo, J.M.; Kong, X.Y. Analyses on the systematic errors of point positioning based on TEQC. *Sci. Surv. Map.* **2007**, *32*, 27–28+34+193. Available online: https://kns.cnki.net/kcms/detail/detail.aspx?FileName=CHKD200704012&DbName=CJFQ2007 (accessed on 10 March 2021).
24. Abou, G.M.; Kaloop, M.R.; Rabah, M.M.; Zeidan, Z.M. Improving Precise Point Positioning Convergence Time through TEQC Multipath Linear Combination. *J. Surv. Eng.* **2018**, *144*, 04018002. [CrossRef]
25. Li, S.W.; Wang, Q.X.; Gong, Y.X. Quality analysis of new signal data of BD-3. *J. Hefei Univ. Technol.* **2021**, *44*, 1111–1117. Available online: https://kns.cnki.net/kcms/detail/detail.aspx?FileName=HEFE202108017&DbName=CJFQ2021 (accessed on 10 March 2021).

26. Ge, T. Quality inspection of measured data of GNSS receiver based on TEQC. *Electron. Technol. Soft. Eng.* **2020**, *14*, 61–62. Available online: https://kns.cnki.net/kcms/detail/detail.aspx?FileName=DZRU202014028&DbName=CJFQ2020 (accessed on 10 March 2021).
27. Guo, H.Y.; Song, F.C.; Qu, Q.X. Analysis of CORS data quality of single base station based on TEQC. *Beijing Surv. Map.* **2019**, *33*, 781–786. [CrossRef]
28. Li, J.; Wang, J.Y.; Xiong, X. Quality Checking and Analysis on GPS Data in Northeast Asia. *Geo. Inform. Sci. Wuhan Univ.* **2006**, *31*, 209–212. Available online: https://kns.cnki.net/kcms/detail/detail.aspx?FileName=WHCH200603004&DbName=CJFQ2006 (accessed on 10 March 2021).
29. Zhang, H.P.; Kong, S.L.; Jiang, Y.M.; Zhou, M.S.; Gao, S.M.; Xu, Y. Efficient Application of GPS Data Preprocessing Based on TEQC. *GNSS World China* **2018**, *43*, 109–114. [CrossRef]
30. Lv, H.; Lv, Z.P.; Cui, Y. Visual development of GNSS data quality analysis software based on TEQC. In Proceedings of the China Satellite Navigation Academic Annual Conference, Beijing, China, 13–15 May 2015. Available online: https://kns.cnki.net/kcms/detail/detail.aspx?FileName=WXDH201505001024&DbName=IPFD2015 (accessed on 10 March 2021).
31. Zhang, P.F. Analysis of GNSS Data Quality of Multi System in Complex Environment. Master's Thesis, Shandong University of Science and Technology, Qingdao, China, 2018. [CrossRef]
32. He, J. Analysis of influence of surface environment on GNSS data quality. Master's Thesis, Chang'an University, Xi'an, China, 2015. Available online: https://kns.cnki.net/KCMS/detail/detail.aspx?dbname=CMFD201601&filename=1015801737.nh (accessed on 10 March 2021).
33. Chen, C.X.; Chen, G.; Wang, Q.P. Data examination and Analysis for Fujian GPS observation network. *Geo. Geodyn.* **2014**, *34*, 17–20. [CrossRef]
34. Wu, C.J.; Hu, Y.K.; Beng, P. Observation quality evaluation and analysis of BDS/GPS. *Beijing Surv. Map.* **2017**, *S1*, 38–42. [CrossRef]
35. He, Y.L.; Wang, Z.W.; Wang, Q.X.; Mao, Y. Data quality analysis of BeiDou global test satellite. *Bull. Surv. Map.* **2018**, *12*, 1–5. [CrossRef]
36. Estey, L.H.; Meertens, C.M. TEQC: The multi-purpose toolkit for GPS/GLONASS data. *GPS Solut.* **1999**, *3*, 42–49. [CrossRef]
37. Hwang, C.; Tseng, T.; Lin, T.; Svehla, D.; Hugentobler, U.; Chao, B.F. Quality assessment of FORMOSAT-3/COSMIC and GRACE GPS observables: Analysis of multipath, ionospheric delay and phase residual in orbit determination. *GPS Solut.* **2010**, *14*, 121–131. [CrossRef]
38. Jäggi, A.; Hugentobler, U.; Beutler, G. Pseudo-Stochastic Orbit Modeling Techniques for Low-Earth Orbiters. *J. Geod.* **2006**, *80*, 47–60. [CrossRef]
39. Zhang, D.Z.; Kong, Q.L.; Zhang, L.G. Precision orbit determination of JASON-3 satellite with on-board GPS at centimeter level. *Sci. Surv. Map.* **2020**, *45*, 42–47. [CrossRef]
40. Xia, Y.W.; Guo, J.Y.; Liu, L.; Kong, Q.L. Research on precise orbit determination of SWARM satellite based on Kinematics and Reduced Dynamics. *Geo. Geodyn.* **2019**, *39*, 392–398. [CrossRef]
41. Dach, R.; Andritsch, F.; Arnold, D.; Vertone, S.; Thaller, D. *Bernese GNSS Software Version 5.2. User manual*; Astronomical Institute, University of Bern, Bern Open Publishing: Bern, Switzerland, 2015.
42. Hu, Z.G.; Zhao, Q.L.; Guo, J. Study on the influence of GPS antenna phase center correction on LEO satellite precise orbit determination. *Acta. Geod. Cartogr. Sin.* **2011**, *40*, 34–38. Available online: http://xb.sinomaps.com/CN/Y2011/V40/ISup./34 (accessed on 10 March 2021).
43. Guo, J.Y. Determination of CHAMP's Orbit and Earth Gravity Model from Onboard GPS Data. Ph.D. Thesis, Shandong of Science and Technology, Taian, China, 2004. Available online: https://kns.cnki.net/KCMS/detail/detail.aspx?dbname=CDFD9908&filename=2004133515.nh (accessed on 10 March 2021).
44. IJssel, J.; Encarnação, J.; Doornbos, E.; Visser, P.N. Precise science orbits for the Swarm satellite constellation. *Adv. Space. Res.* **2015**, *56*, 1042–1055. [CrossRef]